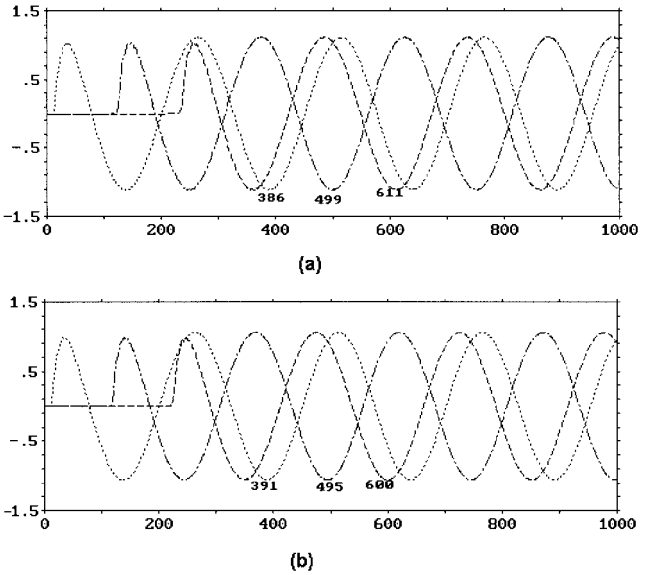

Figure 3 Temporal evolution (a) vacuum and (b) Tellegen medium, magnitude vs. spatial position) of the electric field E_x in three different spatial positions (5010, 5110, and 5210). The time shift of the second minimum, between every case, is shown

between electric and magnetic field is easily obtained from the simulation, and compared with the theoretical one ($180° - \text{arctg}[\sqrt{1-\chi^2}/\chi] = 107.5°$) [8], the error being less than 0.1%. The wave impedance (defined in this case as the relation between the amplitudes of **E** and **H**) is easily obtained, too, and compared with the theoretical value (1, if we use normalized units), being also coincident, with a relative error of less than 0.5%.

Finally, the phase speed of the wave is computed observing the fields in different positions (5010, 5110, and 5210), and the time shift between them (Fig. 3). It agrees well with the normalized theoretical value $v_{\text{theor}} = 1/\sqrt{1-\chi^2} = 1.05\ c$, ($c$ being the phase velocity in vacuum). The velocity obtained in our simulation is $v_{\text{Tellegen}} = 1.07\ c$. The relative error is, then, less than 2%.

ACKNOWLEDGMENT

This work has been partially supported by the Spanish Ministry of Science and Technology, under its project no. TIC 2000-1612-C03-02.

REFERENCES

1. S. Gonzalez García, I. Villó Pérez, R. Gómez Martín, and B. García Olmedo, Extension of Berenger's PML for bi-isotropic media, IEEE Microwave Guided Wave Lett 8 (1998), 297–299.
2. N. Sachdeva, N. Balakrishnan, and S.M. Rao, A new absorbing boundary condition for FDTD, Microwave Optical Technol Lett 25 (2000), 86–90.
3. A. Akyurtlu, D.H. Werner, and K. Aydin: Bi-FDTD: A new technique for modeling electromagnetic wave interaction with bi-isotropic media, Microwave Optical Technol Lett 26 (2000), 239–242.
4. J. Paul, C. Christopoulos, and D.W.P. Thomas, Time-domain modeling of negative refractive index material, Electron Lett 37 (2001), 912–913.
5. I.V. Lindell, S.A. Tretyakov, and M.I. Oksanen, Conductor-backed Tellegen slab as twist polariser, Electron Lett 28 (1992), 281–282.
6. J.A. Kong, Electromagnetic wave theory, Wiley, New York, 1990.
7. K.S. Yee, Numerical solution of initial boundary value problems involving Maxwell's equations in isotropic media, IEEE Trans Antennas Propagat AP-14 (1966), 302–307.
8. I.V. Linden, A.H. Shivola, S.A. Tretyakov, and A.J. Viitanen, Electromagnetic waves in chiral and bi-isotropic media, Artech House, Boston, 1994.

PARTICLE SWARM OPTIMIZATION FOR RECONFIGURABLE PHASE-DIFFERENTIATED ARRAY DESIGN

Dennis Gies and Yahya Rahmat-Samii
Department of Electrical Engineering
University of California, Los Angeles
Los Angeles, CA 90095-1594

Received 24 January 2003

ABSTRACT: *Multiple-beam antenna arrays have important applications in communications and radar. This paper describes a method of designing a reconfigurable dual-beam antenna array using a new evolutionary algorithm called particle swarm optimization (PSO). The design problem is to find element excitations that will result in a sector pattern main beam with low side lobes with the additional requirement that the same excitation amplitudes applied to the array with zero phase should result in a high directivity, low side lobe, and pencil-shaped main beam. Two approaches to the optimization are detailed. First, the PSO is used to optimize the coefficients of the Woodward–Lawson array synthesis method. Second, the element excitations will be optimized directly using PSO. The performance of the two methods is compared and the viability of the resulting designs are discussed in terms of sensitivity to errors in the excitation. Additionally, a parallel version of the particle swarm code developed for a multi-node Beowulf cluster and the benefits that multi-node computing bring to global optimization will be discussed.* © 2003 Wiley Periodicals, Inc. Microwave Opt Technol Lett 38: 168–175, 2003; Published online in Wiley InterScience (www.interscience.wiley.com). DOI 10.1002/mop.11005

Key words: *particle-swarm optimization; reconfigurable array; Woodward–Lawson method*

1. INTRODUCTION

Reconfigurable antenna arrays that are capable of radiating with multiple power patterns using a single power dividing network are desirable for many applications. A number of design methodologies for multiple-pattern arrays have been described in the literature [1, 3]. Solutions to the problem using evolutionary algorithms such as genetic algorithms (GA) and simulated annealing (SA) have also been considered. In this paper we will use the particle swarm optimization (PSO) algorithm to perform dual-beam array optimization.

Previous work has shown the particle swarm to be an effective alternative to more established evolutionary algorithms for certain kinds of problems [8, 9]. Furthermore, the PSO algorithm retains the conceptual simplicity of the genetic algorithm while being much easier to implement and apply to design problems with both discrete and continuous design parameters [7].

The problem described herein is as follows: design a reconfigurable dual-beam 20-element array (see Fig. 1) such that the same amplitude distribution generates either a pencil-shaped or a sector power pattern, the difference being dependent only upon the phase distribution of the array. All excitation phases are set at 0° for the pencil-shaped beam, and are varied in the range $-180° < \theta < 180°$ to form the sector pattern. The design parameters for a particular implementation are summarized in Table 1. Graphically, the patterns should fit within the masks specified in Figures 2 and 3.

In the second section of this paper, the particle swarm optimization algorithm will be reviewed. Relevant material will be discussed to familiarize the reader with the underlying concepts that make the PSO a viable optimization method for antenna synthesis problems. Parallel computing can have an important impact on the amount of time it takes to perform optimizations using the particle

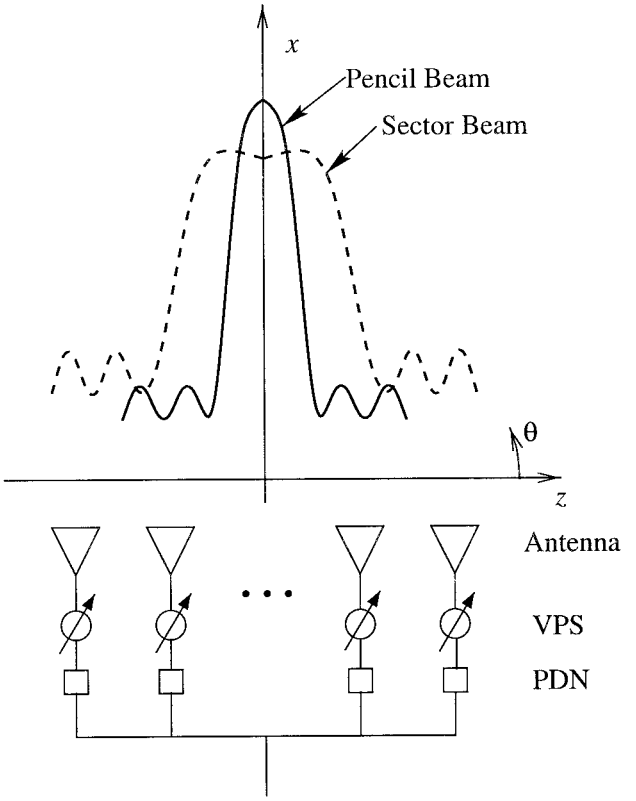

Figure 1 Geometry of the reconfigurable array to be optimized. Each element is attached to a variable phase shifter (VPS) but the power dividing network (PDN) for both the pencil (solid line) and sector (dashed line) beams is the same

swarm. A parallel implementation of the PSO is discussed in terms of the achievable performance gains.

In the third section, the results of two approaches to the dual-beam optimization problem will be presented. The problem was first approached using the Woodward–Lawson beam synthesis method because the current problem is fundamentally one of beam synthesis. In contrast to traditional methods of calculating the Woodward–Lawson coefficients, however, in our case the particle swarm was used to optimize the coefficients. The complexity and additional computational requirements introduced by the Woodward–Lawson method were hypothesized to be unnecessary, and in an attempt to simplify and clarify the process the PSO was used to specify the amplitude and phase of each element's excitation directly.

Finally, the results of the optimizations will be analyzed using independent array simulation software and concepts used to traditionally evaluate the performance of evolutionary optimizers. A sensitivity analysis is also performed to verify that optimized designs could be successfully applied in real-world scenarios.

TABLE 1 Design Parameters for each Beam Pattern

Design Param.	Pencil Pattern	Sector Pattern
SLL	−30 dB	−25 dB
HPBW	6.4°	24°
BW at SLL	20°	40°
Ripple	N/A	0.5 dB

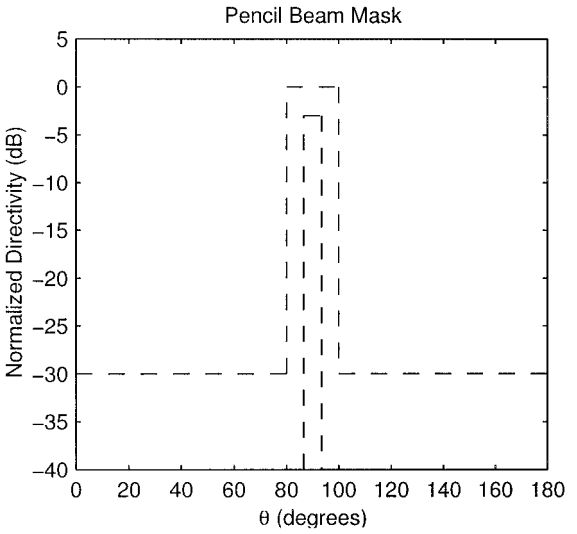

Figure 2 The mask for the pencil-shaped beam shows graphically all of the requirements listed in column 1 of Table 1

2. PARTICLE SWARM OPTIMIZATION

Particle swarm optimization is an evolutionary algorithm similar to genetic algorithms [6] and simulated annealing, but it operates on a model of social interaction between independent agents and utilizes swarm intelligence to achieve the goal of optimizing a problem-specific fitness function [5]. The PSO randomly initializes the position and velocity of each particle within the swarm at the beginning of the optimization. Each position represents a possible solution to the problem, and is specified as the matrix

$$X = \begin{bmatrix} x_{11} & x_{12} & \cdots & x_{1N} \\ x_{21} & x_{22} & \cdots & x_{2N} \\ \vdots & & & \\ x_{M1} & x_{M2} & \cdots & x_{MN} \end{bmatrix}, \quad (1)$$

where M is the number of particles in the simulation and N is the number of dimensions of the problem. Each particle also has an associated velocity, which is a function of the distance from its

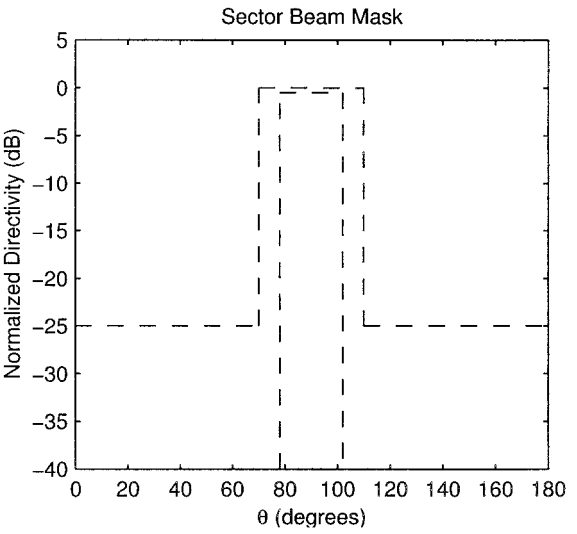

Figure 3 The sector-shaped beam mask specifies a larger beamwidth and a 0.5-dB ripple along the "flat" section of the pattern

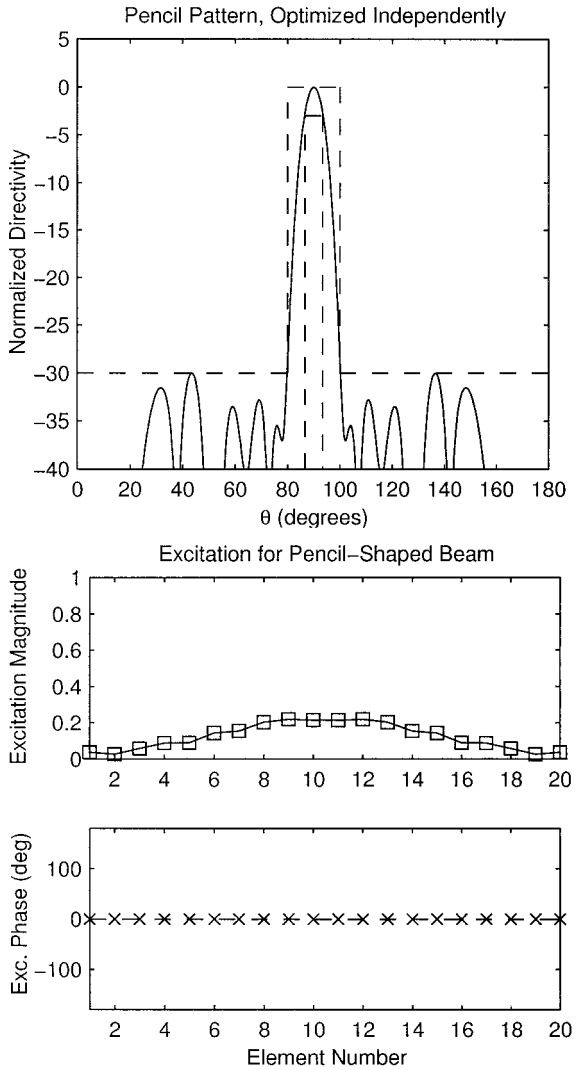

Figure 4 Independently optimized pencil-shaped radiation pattern of a 20-element linear array and the element excitation required to achieve this pattern. Note that the phase is equal to zero for every element in this case

current position to the positions which have previously resulted in a good fitness value. The velocity matrix must be the same size as the position matrix, and is represented as

$$V = \begin{bmatrix} v_{11} & v_{12} & \cdots & v_{1N} \\ v_{21} & v_{22} & \cdots & v_{2N} \\ \vdots & & & \\ v_{M1} & v_{M2} & \cdots & v_{MN} \end{bmatrix}. \tag{2}$$

In order to update the velocity matrix at each iteration of the algorithm, every particle must also "know" the global best and personal best position vectors. The global best-position vector specifies the location in solution space at which the best fitness value was obtained. The global best may be attained by any particle at any iteration up to the present one. Similarly, the personal best-position vector specifies the position at which any given particle achieved its best fitness value up to the current iteration. Therefore, although every particle in the swarm accesses the same global best position, the personal best positions are specific to a given particle. The personal best positions can also be represented by an $M \times N$ matrix:

$$P = \begin{bmatrix} p_{11} & p_{12} & \cdots & p_{1N} \\ p_{21} & p_{22} & \cdots & p_{2N} \\ \vdots & & & \\ p_{M1} & p_{M2} & \cdots & p_{MN} \end{bmatrix}. \tag{3}$$

The global best position is an N-dimensional vector given by

$$G = [g_1 \quad g_{12} \quad \cdots \quad g_N]. \tag{4}$$

X, V, P, and G together contain all of the information required by the particle-swarm algorithm. The heart of the algorithm, however, is the process by which these matrices are updated on each successive iteration. In an effort to numerically model the behavior of groups of natural agents such as fish or birds, the algorithm requires that the position of each particle should move towards both the global best and its personal best positions. For this to occur, the velocity of the particle must be appropriately chosen. The velocity matrix is updated each iteration according to [4]:

$$v_{mn} = v_{mn} + c_1\eta_1(p_{mn} - x_{mn}) + c_2\eta_2(g_n - x_{mn}), \tag{5}$$

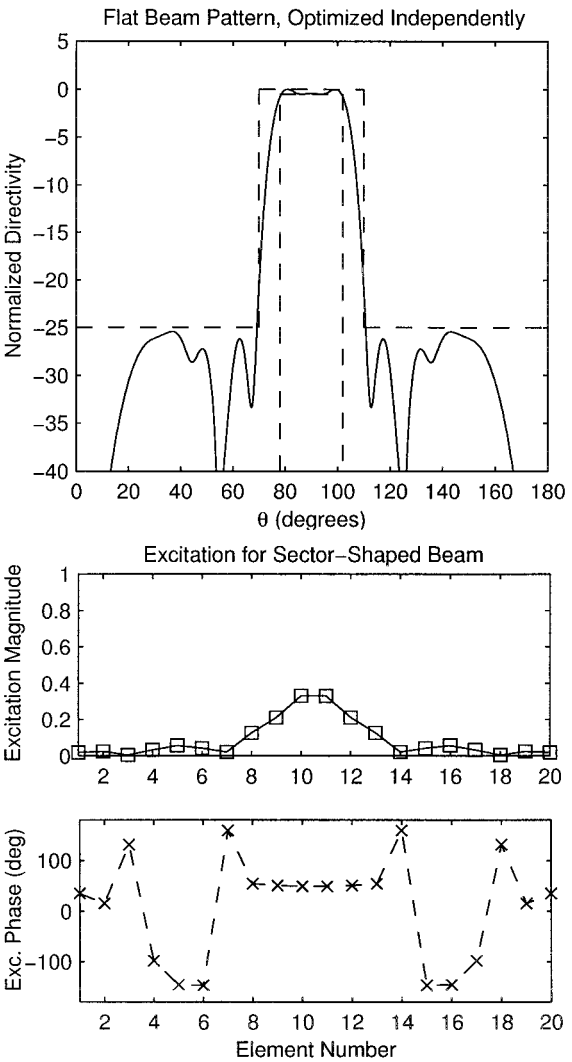

Figure 5 Independently optimized sector-shaped radiation pattern of a 20-element linear array and the element excitation required to achieve this pattern. Note that both amplitude and phase are optimized by the PSO in this case

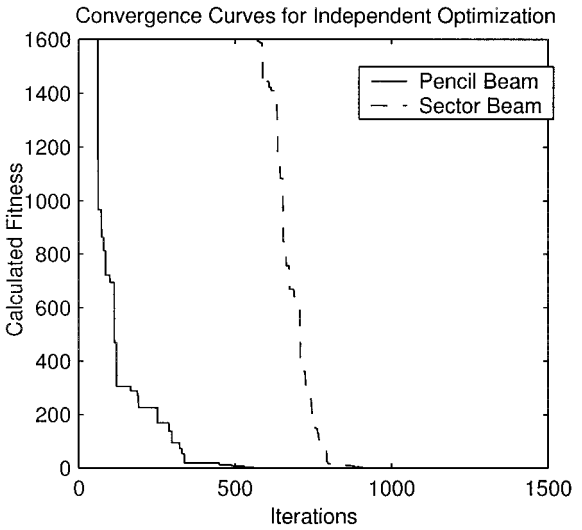

Figure 6 Convergence curves of the single-beam optimizations show that the sector pattern is significantly more difficult to optimize than the pencil pattern

where η_1 and η_2 are uniform random variables in the range $0 < \eta_{1,2} < 1$. For every dimension, the particles move in the direction specified by the velocity matrix according to a simple relationship given by

$$X = X + V. \tag{6}$$

For the problem at hand, the number of dimensions is equal to twice the number of antenna elements because both the amplitude and phase of each parameter must be specified by the PSO. Also, a swarm of 20 particles was used. The algorithm parameters c_1 and c_2 specify the relative weight that the global best position has versus the particle's personal best. Empirical testing has found 2.0 to be a reasonable value for both c_1 and c_2 [4] for swarms that are not subject to a constriction factor as described in [2]. Linear velocity damping was applied with the upper limit 0.9 and the lower limit 0.4. Velocity damping improves the convergence behavior of the particle swarm by gradually increasing the relative emphasis of the global and personal best positions on a particle's velocity.

2.1 Fitness Evaluation

Evolutionary algorithms use the concept of fitness to represent how well an arbitrary solution satisfies the design parameters. Each of the parameters used to calculate the fitness is referred to as a fitness factor. The fitness factors must together quantify the solution. For antenna problems, common fitness factors are directivity, gain, SLL, and physical size and weight.

For the reconfigurable dual-beam optimization, the fitness function must quantify the entire array radiation pattern. One possible method of doing so would be to compare the calculated pattern point-by-point with the desired pattern as follows

$$\text{Fitness} = \int_0^{\pi} |f_d(\theta) - f(\theta)| d\theta. \tag{7}$$

In practice, this method does not work well because the optimization tries to maximize the nulls between adjacent side lobes in addition to minimizing the side-lobe peaks. In essence, this wastes optimization power because the nulls between side lobes are of little importance to the performance of most antenna arrays.

Instead, the calculated pattern can be described in terms of the criteria of the desired pattern. This method requires considerably more finesse because no assumptions can be made regarding the shape of the calculated pattern. If any of the parameters listed in Table 1 are left out of the calculation, the optimization will almost certainly result in very poor designs.

The fitness function for the dual-beam array optimization can be expressed as follows:

$$\text{Fitness} = \sum_{i=1}^{3} (P_{i,d}^{(p)} - P_i^{(p)})^2 + \sum_{i=1}^{4} (P_{i,d}^{(s)} - P_i^{(s)})^2, \tag{8}$$

where the superscript p specifies fitness factors for the pencil pattern and the superscript s specifies fitness factors for the sector pattern. The subscript d represents the desired values for each fitness factor. Finally, P represents the applicable fitness factors specified in Table 1. Essentially, the first summation is performed

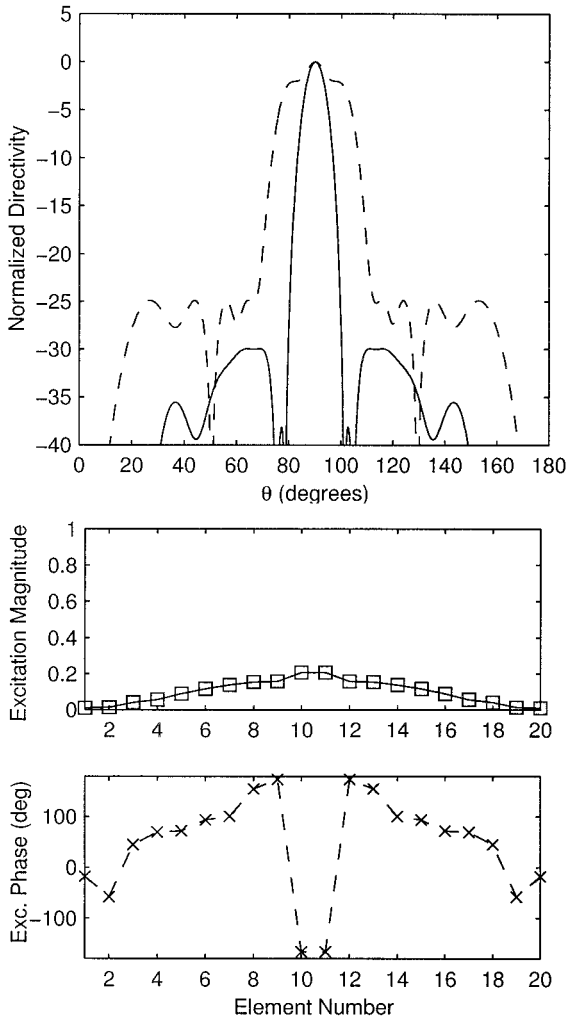

Figure 7 Dual-beam pattern achieved by using the PSO to optimize the sample values used as input to the Woodward–Lawson method. The pencil beam is shown with a solid line and the sector pattern with a dashed line. Also shown are the element excitations that produce the dual-beam pattern. The phases of the array generating the pencil-shaped beam are all equal to zero

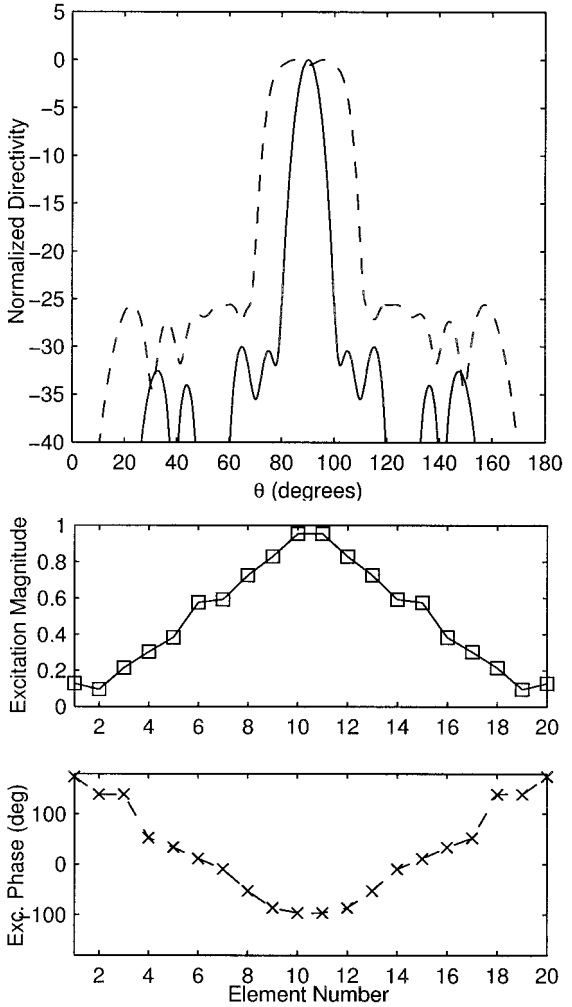

Figure 8 Dual-beam pattern achieved by using the PSO to optimize the element excitation amplitude and phase directly. Below are the element excitations that produce the dual-beam pattern. Again, the phases of the array generating the pencil-shaped beam are all equal to zero

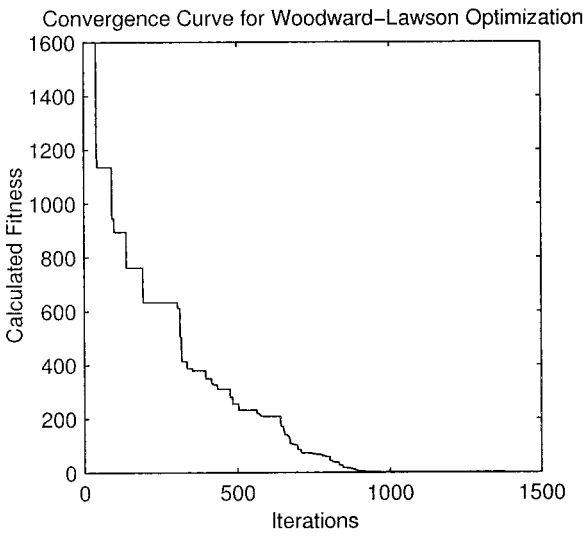

Figure 9 Convergence curve of the dual-beam optimization achieved by varying the Woodward–Lawson coefficients using PSO

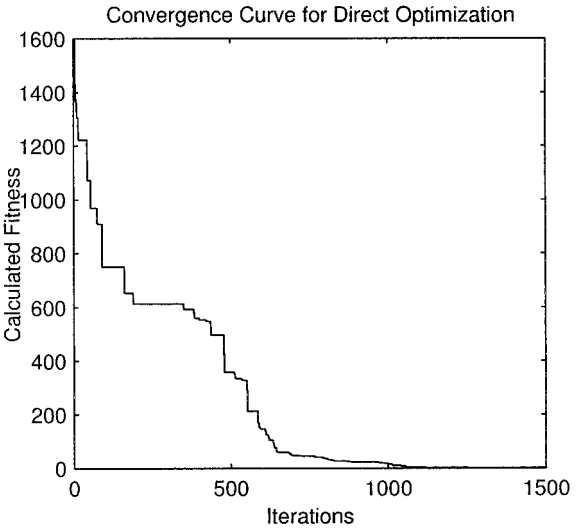

Figure 10 Convergence curve of the dual-beam optimization achieved by varying the element excitations (both amplitude and phase) directly using PSO

over the first column of Table 1, and the second summation is performed over the second column. Unlike the fitness value for the pencil beam pattern (which requires just three fitness factors), the sector pattern fitness must also take into account the pattern ripple. This explains the difference in the limits of the two summations.

2.2 Parallel Particle Swarm Optimization

The particle swarm algorithm maps well to the parallel computing paradigm. Because the vast majority of the computing time required for a global optimization is involved in simulating the antenna structure, it is much more efficient to run multiple simulations simultaneously on the nodes of a Beowulf cluster than to run the simulations serially on a workstation.

The particle swarm algorithm is parallel by nature since each particle can be thought of as an independent agent. At the beginning of any given iteration, each particle has all the information it needs to determine its current fitness. At the end of each iteration, the agents exchange some information, update their positions in solution space, and run another simulation. Parallel computing benefits the particle swarm by providing each agent with its own processor on which to run the simulations.

In theory, a parallel version of the particle swarm could perform M times better than the serial version, where M is the number of particles used in the simulation. In practice, message passing and computational overhead make the parallel version less than perfectly efficient. For the dual-beam problem, a parallelized particle swarm converged on a solution approximately 8 times faster than the serial counterpart when a swarm of 10 agents were used. The optimization was run on a Beowulf cluster of 5 nodes, each with two processors. The performance of the parallel version could likely be improved by further optimizing the code to minimize the amount of data passed between nodes.

3. DETERMINATION OF EXCITATION COEFFICIENTS

3.1 Independent Optimization of Both Patterns

To verify that the optimization code and fitness evaluation routines were operating correctly, both of the desired radiation patterns were synthesized using the PSO independently. The fitness was calculated using only the $P^{(p)}$ or $P^{(s)}$ terms, depending on which

TABLE 2 Sensitivity to Error in Excitation Amplitude

	Pencil Pattern, % Change			Sector Pattern, % Change			
Max. Error (%)	SLL	3 dB BW	30 dB BW	SLL	3 dB BW	25 dB BW	Ripple
1	0.10	0.00	0.55	0.30	0.55	0.00	0.03
2	0.21	0.00	0.62	0.71	0.82	0.04	0.28
3	0.72	0.00	0.95	0.75	0.67	0.07	0.43
4	0.27	0.00	1.05	1.48	0.55	0.20	0.77
5	0.73	0.00	0.73	1.67	0.70	0.16	0.86
6	1.36	0.00	0.98	1.73	0.39	0.18	0.17
7	2.14	0.00	0.69	2.41	0.30	0.32	2.01
8	1.38	0.00	0.76	2.89	0.91	0.09	0.58
9	1.13	0.00	0.91	3.51	0.76	0.02	0.47
10	2.76	0.00	0.69	3.70	0.76	0.04	1.60
11	2.89	0.00	0.40	3.78	0.73	0.11	2.55
12	2.57	0.10	0.84	4.25	0.61	0.02	2.34
13	4.58	0.00	0.73	3.84	1.00	0.21	2.63
14	3.35	0.00	0.51	4.34	0.85	0.14	0.85
15	3.32	0.30	0.51	5.60	1.73	0.52	4.61

pattern was desired. Figures 4 and 5 show the resulting radiation patterns for optimized 20-element arrays along with the element excitation amplitudes and phases.

It is also instructive to examine the convergence curves of the independently optimized patterns. Convergence curves are often used to graphically show how quickly a global optimization algorithm can converge to a solution of a certain problem. From Figure 6 it is clear that the sector-shaped pattern is difficult to optimize because it requires many more iterations than the pencil-shaped pattern before the fitness value approaches the optimum. Because the fitness function has been described as the difference between the desired and actual radiation patterns, this implementation of the particle swarm attempts to minimize the fitness value, hence the optimal fitness is zero.

3.2 Optimization of the Woodward–Lawson Coefficients

The first attempt to concurrently design a dual-beam array utilized the Woodward–Lawson method to calculate the array factor and radiation pattern. The Woodward–Lawson method requires as input sample values of the desired array factor given by

$$a_n = f_d(w_n), \tag{9}$$

where f_d is the desired pattern and the sample points, w_n are given by

$$w_n = n\,\frac{\lambda}{Pd} = \frac{n}{L/\lambda}, \tag{10}$$

where P is the number of elements, d is the element spacing, and $L = Pd$ is the overall length of the array. Also, $|n| \le M$ (M being the number of samples of the desired pattern) and $|w_n| \le 1.0$. Given these samples of the desired pattern, the element excitations of the array are calculated from

$$I_m = \frac{1}{P}\sum_{n=-M}^{M} a_n e^{-j2\pi(z_m/\lambda)w_n}, \tag{11}$$

where z_m is the location along the z-axis of the m^{th} element. The array factor can thus be easily calculated from

$$AF = \sum_{n=0}^{P-1} I_n e^{j\beta n d\cos\theta}. \tag{12}$$

TABLE 3 Sensitivity to Error in Excitation Phase

	Pencil Pattern, % Change			Sector Pattern, % Change			
Max. Error (%)	SLL	3 dB BW	30 dB BW	SLL	3 dB BW	25 dB BW	Ripple
1	0.00	0.00	0.00	0.52	0.82	0.02	3.83
2	0.00	0.00	0.00	1.29	2.70	0.54	8.71
3	0.00	0.00	0.00	1.95	3.82	0.80	10.61
4	0.00	0.00	0.00	2.75	5.06	1.14	14.68
5	0.00	0.00	0.00	3.00	6.48	1.82	19.43
6	0.00	0.00	0.00	4.14	7.61	2.27	23.37
7	0.00	0.00	0.00	4.63	7.73	2.32	24.42
8	0.01	0.00	0.00	6.87	9.45	3.18	31.81
9	0.01	0.00	0.00	7.49	10.45	4.20	41.33
10	0.01	0.00	0.00	9.09	11.85	4.89	51.29
11	0.01	0.00	0.00	9.88	12.70	6.86	55.50
12	0.01	0.00	0.00	9.50	13.58	8.54	60.71
13	0.02	0.00	0.00	10.04	15.06	10.84	72.74
14	0.02	0.00	0.00	11.45	15.24	13.36	76.85
15	0.03	0.00	0.00	12.55	16.12	14.46	86.91

The PSO was used to optimize the sample values required as input for the Woodward–Lawson method. The fitness evaluation program, taking w_n as input from the PSO, calculates the element excitations, I_n, and subsequently the radiation pattern.

Acceptable results were achieved using this method. As Figure 7 shows, both patterns can be generated by the excitation shown (recall that the phases of the excitation for the pencil beam are all equal to zero).

3.3 Optimization of the Element Excitations

Performing the optimization on the element excitations directly provides certain benefits over the Woodward–Lawson synthesis technique described previously. (Direct optimization of the element excitations is shortened to "direct method" for the remainder of this paper.) One benefit of the direct method is that the number of dimensions is reduced by two in the case of an array with an even number of elements. This is true because the Woodward–Lawson method requires a sample point at $z = 0$, where there is not an array element.

The direct method provides only a negligible performance benefit over the Woodward–Lawson method, but the complexity of the program was reduced significantly. Also, the direct method still provides very good results. Figure 8 shows the dual-beam radiation patterns and the element excitations.

It should be noted that although the radiation patterns of Figures 7 and 8 are very similar, their excitations are vastly different. This illustrates one of the ways in which evolutionary algorithms are powerful; they can provide numerous acceptable solutions to the same problem, allowing the designer to choose among them using more subjective requirements than those specified in the fitness function.

4. CONVERGENCE AND SENSITIVITY STUDIES

4.1 Convergence

Figures 9 and 10 show the convergence curves and Figure 11 shows the numerical simulation of the optimization of the element excitations and of the Woodward–Lawson coefficient optimization using the PSO, the convergence for both methods is similar. Optimal solutions are first reached at about 1000 iterations of the PSO. In contrast, the PSO needed 800 iterations to find optimal solutions for the independent sector pattern. Even easier to optimize was the independent pencil pattern, which required only 300 iterations. None of these results defy expectation. Evolutionary algorithms all require more time to solve more difficult problems. In this sense, the most difficult problems are those with more design parameters. The small difference between the number of iterations it takes to optimize the sector pattern versus the dual-beam pattern illustrates that the number of dimensions has not increased, rather, the solution space is more complicated, and thus harder to optimize. Similarly, the parallel version of the particle swarm converges in approximately the same number of iterations as the serial version, although it does so in less physical time.

4.2 Design Sensitivity

In certain implementations of dual-beam antenna arrays, the element excitations may not be exactly the same as the design calls for. Error may be introduced by the power dividing network or the phase shifting components. In particular, digital phase shifters only guarantee accuracy within a certain range depending on the number of bits available for phase discretization. A parameter sensitivity analysis was performed to evaluate how the dual-beam designs achieved by the particle swarm would operate under realistic conditions. Because the array parameters are so finely tuned, there is reason to be concerned that even a small change in the element excitations could induce a significant change in the radiated power pattern. Our simulations show that this is not the case.

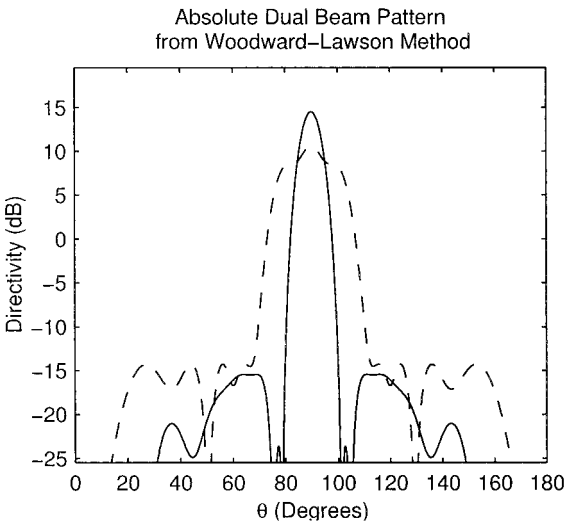

Figure 11 A numerical simulation verifies the results of the PSO design and provides a sense of the directivities of each beam relative to one another. This figure shows the results of the optimization of the Woodward–Lawson coefficients

Tables 2 and 3 show the results of a sensitivity analysis of the amplitude and phase of the element excitations, respectively. Each column of the tables tracks one of the seven design parameters. Each row shows the average value of the parameter over 50 runs. Each of the 50 runs applied a random error to either the optimized amplitude or phase of each array element. The magnitude of the error was randomly chosen but does not exceed $n\%$ of the optimized value, where n is specified in the first column of each table.

A few significant conclusions can be drawn from this data. Most importantly, it is clear that the radiated power patterns are much more sensitive to errors in the phase than errors in amplitude. The SLL of the sector pattern is more than 3.75-dB higher than the specification when the maximum phase error is 15%. However, a common 6-bit phase shifter will have a maximum error of 6°, which is about 1.67%. Table 3 clearly shows that for that level of uncertainty, the sector pattern will still be acceptable for most applications.

4.3 Verification of Results

More information about the optimized designs was obtained by simulating the arrays with a comprehensive array simulation program developed at UCLA. The program provides a measure of the absolute directivity of the array, which the methods previously described cannot. Figure 12 shows the radiation patterns for the PSO-generated design of Figure 8. The directivities of the patterns are as expected over the range $0 \leq \theta \leq 180$.

5. CONCLUSION

This research has taken advantage of the flexibility of the particle swarm optimization technique by applying it to the problem of reconfigurable multiple-beam array synthesis. The ease with which the PSO can be applied to problems in electromagnetics and antennas make it a useful and promising tool for researchers. The performance of the algorithm compares well to other techniques that have been applied to this problem, in particular the global optimization methods of genetic algorithms and simulated anneal-

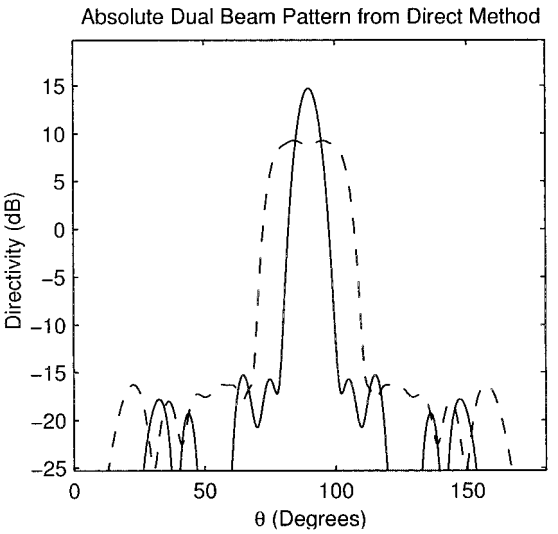

Figure 12 This figure verifies the pattern achieved by directly optimizing the element excitations

ing. The particle swarm was used to find solutions to a specific dual-beam array problem in two ways. First, the PSO optimized the Woodward–Lawson coefficients. Second, the PSO optimized the element excitation amplitudes and phases directly. Both methods provided acceptable solutions to the problem, but the second method was found to be more straightforward both conceptually and in practice.

In real-life applications, errors in power dividing networks and sampling error associated with binary phase shifters are inevitable, and practical arrays must be able to maintain acceptable performance in spite of these imperfections. The particle swarm-optimized reconfigurable array designs were found to be resistant to simulated variations in the excitation coefficients.

Future work with the particle swarm might extend to many different areas of antenna design and analysis. The PSO program developed at UCLA has the ability to be linked to nearly any numerical simulation program available, and is therefore capable of optimizing any structure that can be numerically simulated. In particular, multiple-beam array problems could be approached using more degrees of freedom than are utilized in the present work. For example, the element position and geometry could be optimized in addition to the array excitation to achieve even more complex multiple-beam patterns.

REFERENCES

1. O.M. Bucci, G. Mazzarella, and G. Panariello, Reconfigurable arrays by phase-only control, IEEE Trans Antennas Propagat 39 (1991), 919–925.
2. M. Clerc and J. Kennedy, The particle swarm: Explosion, stability, and convergence in a multidimensional complex space, IEEE Trans Evolutionary Computation 6 (2002), 58–73.
3. M. Durr, A. Trastoy, and F. Ares, Multiple-pattern linear antenna arrays with single prefixed distributions: Modified Woodward–Lawson synthesis, Electron Lett 26 (2000), 1345–1346.
4. R.C. Eberhart and Y. Shi, Particle swarm optimization: Developments, applications, and resources, Proc 2001 Conf Evolutionary Computation 1 (2001), 81–86.
5. J. Kennedy and R. Eberhart, Particle swarm optimization, vol. IV, 1995, pp 1942–1948.
6. Y. Rahmat-Samii and E. Michielssen, Electromagnetic optimization by genetic algorithms, John Wiley & Sons, 1999.
7. J. Robinson and Y. Rahmat-Samii, Particle swarm optimization in electromagnetics, IEEE Trans Antennas Propagat (2002), Submitted for publication.
8. J. Robinson, S. Sinton, and Y. Rahmat-Samii, Particle swarm, genetic algorithm, and their hybrids: Optimization of a profiled corrugated horn antenna, San Antonio, Texas, 2002.
9. Y. Shi and R.C. Eberhart, Empirical study of particle swarm optimization, July 6–9 1999, pp 1945–1950.

THIN ABSORBING STRUCTURE FOR ALL INCIDENCE ANGLES BASED ON THE USE OF A HIGH-IMPEDANCE SURFACE

S. A. Tretyakov and S. I. Maslovski
Radio Laboratory
Helsinki University of Technology
P. O. Box 3000
FIN-02015 HUT, Finland

Received 21 January 2003

ABSTRACT: *It is shown that thin mushroom layers (high-impedance surfaces realized as regular arrays of small patches at a small distance from a metal surface) can be used as radar-absorbing structures whose performance does not change with the incidence angle for TM-polarized waves. The key role of the vias connectors between the patches and the ground plane is explained, and potential performance demonstrated in examples.*
 Microwave Opt Technol Lett 38: 175–178, 2003; Published online in Wiley InterScience (www.interscience.wiley.com). DOI 10.1002/mop.11006

Key words: *absorbers; RCS reduction; high-impedance surface; mushroom layer*

1. INTRODUCTION

The design of thin absorbing layers for radar cross section reduction is a challenging task, because the thickness reduction leads to a decrease of the bandwidth [1]. Another problem is that obliquely incident waves are absorbed much less effectively than normally incident plane waves. Indeed, imagine an absorbing layer excited by a plane wave whose tangential to the interface wavevector component is $\mathbf{k}_t$. If the absorber material has the material parameters ε and μ, the normal to the surface component of the propagation factor is $\beta = \sqrt{k^2 - k_t^2}$, where $k = \omega\sqrt{\varepsilon\mu}$. For plane waves coming from free space (parameters denoted as ε_0, μ_0, $\eta_0 = \sqrt{\mu_0/\varepsilon_0}$, $k_0 = \omega\sqrt{\varepsilon_0\mu_0}$) at an angle θ the tangential propagation factor is $k_t = k_0 \sin\theta$. Thus, the electrical thickness of the layer $|\beta|d$ decreases if the incident angle increases. Due to the same reason, the resonance frequency of Salisbury absorbers (resistive sheets located quarter-wavelength apart from metal bodies) is different for different incidence angles: the electrical thickness of the spacing between the sheet and the conductor is proportional to $\cos\theta$.

In this paper we describe an absorbing layer that does not suffer from this drawback, and has the same performance for wide ranges of the incidence angles.

2. HIGH-IMPEDANCE MUSHROOM SURFACES FOR OBLIQUELY INCIDENT WAVES

The proposed design is based on the use of a certain feature of high-impedance surfaces realized as so-called mushroom layers: